Journal of The Electrochemical Society, **152** (10) A2017-A2022 (2005)
0013-4651/2005/152(10)/A2017/6/$7.00 © The Electrochemical Society, Inc.

Oxygen Reduction by Sol-Derived Pt/Co-Based Alloys for PEM Fuel Cells

Jeff N. Soderberg,[a] Aislinn H. C. Sirk,[a] Stephen A. Campbell,[b,*] and Viola I. Birss[a,*,z]

[a]*Department of Chemistry, University of Calgary, Calgary, Alberta, Canada T2N 1N4*
[b]*Ballard Power Systems, Burnaby, British Columbia, Canada V5J 5J9*

A route toward the synthesis of several Pt/Co-based catalysts for the oxygen reduction reaction (ORR) in proton exchange membrane (PEM) fuel cells is described here. The composition of these catalysts has been determined by X-ray diffraction studies, while their electrochemical activity was established using slow sweep cyclic voltammetry in 0.5 M H_2SO_4 at room temperature. We have found that by mixing a Co oxide sol precursor with Pt supported on carbon (Pt/C), followed by heat-treatment at 700 or 900°C, the active PtCo alloy catalyst is formed. In contrast, when exactly the same procedure is followed but a Co oxide sol-derived Co/N/C catalytic material is employed, Pt_3Co alloy catalysts, which are somewhat less active toward the ORR, are formed. Catalysts formed by heating at 900°C are more active than those formed at 700°C, and all of our Pt/Co catalysts are more active toward the ORR than pure Pt on carbon.
 [DOI: 10.1149/1.2018207]

Manuscript submitted February 24, 2005; revised manuscript received May 26, 2005. Available electronically August 25, 2005.

Hydrogen-fueled proton exchange membrane (PEM) fuel cells demonstrate great promise as future energy sources, as they convert chemical energy to electrical energy with a significantly greater efficiency than in standard combustion processes. Furthermore, as PEM fuel cells run on clean H_2 at low temperatures (below 100°C), they produce no particulates, NO_x, SO_x, or CO_2, and are therefore considered to be environmentally friendly. The only by-products of the PEM fuel cell are heat and water. However, the widespread commercialization of PEM fuel cells has been hindered by a number of factors, including the challenges of implementing a hydrogen infrastructure, the cost of fuel cell manufacturing, and limitations in terms of fuel cell performance and durability.

Currently, both the anode and cathode electrocatalysts in the PEM fuel cell are composed of Pt distributed on a high-surface-area carbon support. While H_2 oxidation is kinetically rapid at the Pt anode, a significant voltage loss occurs at the Pt cathode, as the kinetics of the O_2 reduction reaction (ORR) are extremely sluggish, even at Pt catalysts. Therefore, there is a substantial effort currently underway to develop an alternative, more efficient, and lower cost cathode electrocatalyst for the ORR in PEM fuel cells.

One promising area of investigation has involved the alloying of Pt with transition metals such as Co,[1-13] Ni,[7,10,14] Cr,[1,5] Co–Cr,[2,6] and Co–Ni.[8,9] Many of these catalysts were initially developed for the ORR in phosphoric acid fuel cells[15] but have also been found to perform well in PEM fuel cells, giving reported enhancements in activity of as much as five times.[1,10,11] A number of explanations for the improvement in activity by the addition of less noble metals to Pt have been given, including the lowering of the Pt oxidation state,[6] the suppression of Pt oxide formation,[6,9] the formation of a new electronic structure with higher Pt 5d orbital vacancies,[5] a decrease in the Pt–Pt distance, and therefore a more favorable adsorption of O_2,[5] and the formation of a catalytic, thin Pt skin on the surface of the alloy.[3,4,11]

Another avenue of pursuit in replacing pure Pt cathodes has involved the use of N- and C-containing metal (Co, Fe, etc.) macrocycles, which after heat-treatment to 500–1000°C in an inert atmosphere, also produce active, fairly stable ORR catalyst materials.[16] This heat-treatment step is known to partially or completely break down the macrocyclic ring, although the nature of the active sites which result are still the subject of much debate.[17] It has further been demonstrated that simpler Fe-[18,19] and Co-based precursors[20-23] can yield good ORR electrocatalysts, as long as C and N are also present. Methods that have been used to prepare such catalysts include sputtercoating Co and C together in a N_2 atmosphere,[23] incorporation of anionic Co species into an oxidized polypyrrole film,[20] heat-treatment of Co salts on carbon powder,[22] and electric arc production of carbon-coated Co nanocrystallites[21] under flowing acetonitrile.

In this direction, we have recently synthesized some promising ORR catalysts using a Co oxide sol as the starting material, followed by the addition of relatively simple N- and C-containing ligands, such as ethylenediamine or 1,2-phenylenediamine[24-26] into the sol, and then heat-treating these materials under a N_2 atmosphere together with carbon powder. These Co oxide sol-derived catalysts were found to be more active toward the ORR than any previously reported Co-based catalysts. However, while the cost of these catalysts is clearly significantly lower than Pt (500–1000x), their activity is still less than Pt and less than required for many applications.

Therefore, the primary goal of this work was to combine our sol-derived Co-based catalyst with Pt and to determine whether any synergistic catalytic effects or unique catalytic materials could be generated. We have found that by mixing the Co oxide sol precursor with Pt supported on carbon (Pt/C), followed by heat-treatment at 700 or 900°C, active PtCo alloy catalysts are formed. In contrast, when exactly the same procedure is followed but the Co oxide sol is replaced by an equivalent molar quantity of our Co oxide sol-derived Co/N/C catalytic material, Pt_3Co alloy catalysts which are somewhat less active toward the ORR result. We therefore report here on the synthesis, characterization, and evaluation of these Pt/Co-containing materials as catalysts for the ORR, showing also that catalysts are more active when formed at 900 vs 700°C.

Experimental

Synthesis of Co-based percursors (Ref. 24, 26).—4.4 g of $Co(NO_3)_2{\cdot}6H_2O$ were dissolved in 15 mL of absolute ethanol and refluxed (74°C) for 6 h, followed by 18 h of stirring at room temperature. 15 mL of ethyl acetate was then added to prepare a 0.5 M Co oxide sol precursor.[27] A 1 mol equiv solution of ethylenediamine (en) or 1,2-phenylenediamine (phen) was added dropwise as a 10% w/w solution (en) or a 0.5 M solution (phen) in 1:1 ethanol:ethyl acetate to a refluxing, stirring solution of the Co oxide sol over 6 h. After removal of the precipitate,[26] two more equivalents of ligand were added. The resulting Co-containing precursor solutions, ranging in concentration from 0.1 to 0.5 M Co, are referred to as Co oxide-en and Co oxide-phen sols, distinguishing them from the original, pure Co oxide sol.

20% Pt/C powder (Johnson Matthey) was used as the Pt source for the synthesis of the three Pt/Co catalysts under study here (Table I). The three Co sol-based precursors (Co oxide sol, Co oxide-en, and Co oxide-phen) were applied directly to the Pt/C powder by

* Electrochemical Society Active Member.
z E-mail: birss@ucalgary.ca

Table I. Details of synthesis of Pt/Co catalysts[a].

Catalyst type	Co sol-based precursor	Volume of Co precursor[a] added (mL)	Weight of 20% Pt/C powder (g)
Pt/Co-I	Co oxide sol (3.03 M)	0.100	0.2964
Pt/Co-II	Co oxide-en (0.17 M)	0.500	0.0807
Pt/Co-III	Co oxide-phen (0.151 M)	1.500	0.2208

[a] The three Pt/Co catalysts were synthesized by supporting the Co sol-based precursor on Pt/carbon powder, then heating for 2 h to either 700 or 900°C, and then mixing with Nafion as a binding agent.

incipient impregnation,[28] with the metal components adjusted to give a 1:1 Pt:Co atomic ratio. The resulting mixture was allowed to dry in air at room temperature before heat-treatment (see the following section). For comparison purposes, the Co sol-based precursors (Table I), without any Pt, were also applied directly to activated carbon powder (Vulcan XC72R, Cabot Corp.) and allowed to dry at room temperature in air.

Procedure for heat-treatment (Ref. 24, 26).— The C-supported catalyst powders, placed in a quartz tube, first sat under a flow of N_2 for at least 1 h prior to being moved into a preheated tube furnace. The temperature was then held at either 700 or 900°C for 2 h, after which the samples were removed from the furnace and allowed to cool, all under a flow of N_2. The three heat-treated Pt/Co catalysts, arising from the three different Co sol precursors dispersed on Pt/C powder, are coded as follows for the remainder of this paper: Co oxide sol-based catalyst: Pt/Co-I; Co oxide-en: Pt/Co-II; Co oxide-phen: Pt/Co-III (Table I).

Preparation of catalyst/Nafion suspension Ref. 24, 26.— An 11% (w/w) Nafion solution (EW 1100) was diluted with absolute ethanol to give a 1% (w/w) Nafion mixture and was then mixed in a 1:1 dry weight ratio with the C powder-supported catalysts and precursors. The suspension was sonicated for ~15 min before application to the electrode.

Electrochemical assessment of catalysts and determination of ORR activity.—A 7 mm diam glassy carbon (GC) rotating disk electrode (RDE) was used to test for the ORR activity of the catalysts (Pt/Co-I, Pt/Co-II, and Pt/Co-III, as well as the precursors, Co oxide sol, Co oxide-en, Co oxide-phen, and the pure Pt/C powder). A three-electrode electrochemical cell was used, containing a mesh counter electrode (Pt or Pt black) and a reversible hydrogen electrode (RHE) reference electrode. The cell solution of 0.5 M H_2SO_4 was first purged with vigorously bubbling N_2 or O_2 and then maintained under a N_2 or O_2 atmosphere at a flow rate of 36 mL/min during the electrochemical measurements.

To apply the sonicated Nafion-containing suspension to the electrode disk, a micropipette was used for a controlled volume application (14 μL), resulting in a loading ranging from 0.12 to 0.14 mg/cm^2 of Pt. This Pt loading is within the normal range reported in the literature, typically 0.1–1.0 mg/cm^2,[1,2,5,8,9,29] although loadings as low as ~0.014 mg/cm^2[10] have also been employed. The electrode was then dried at room temperature for approximately 15 min before drying at 105°C for 10 min, all in air.

Cyclic voltammograms (CVs) were collected in a N_2-purged aqueous solution at 25°C with no electrode rotation[c] to obtain a baseline for comparison to the ORR data. The standard test regime involved cycling the potential between 0.05 and 1.1 V at 10 mV/s until a steady-state signal was obtained. The cell was then saturated with O_2, as described above, and a CV was run at 10 mV/s at different rotation rates (0–2000 rpm) using a Pine analytical rotor (model ASR-2). The RDE measurements were carried out with an EG&G PARC 175 function generator used in conjunction with a Hokuto Denko HA-301 potentiostat. The electrochemical data were recorded by computer software (Chart4 by PowerLab). All samples were subjected to duplicate or triplicate electrochemical tests.

[c]Rotation of the electrode did not change the electrochemical response in N_2-purged 0.5 M H_2SO_4, except to introduce some noise and a small ORR signal due to leakage of O_2 into the cell with prolonged rotation.

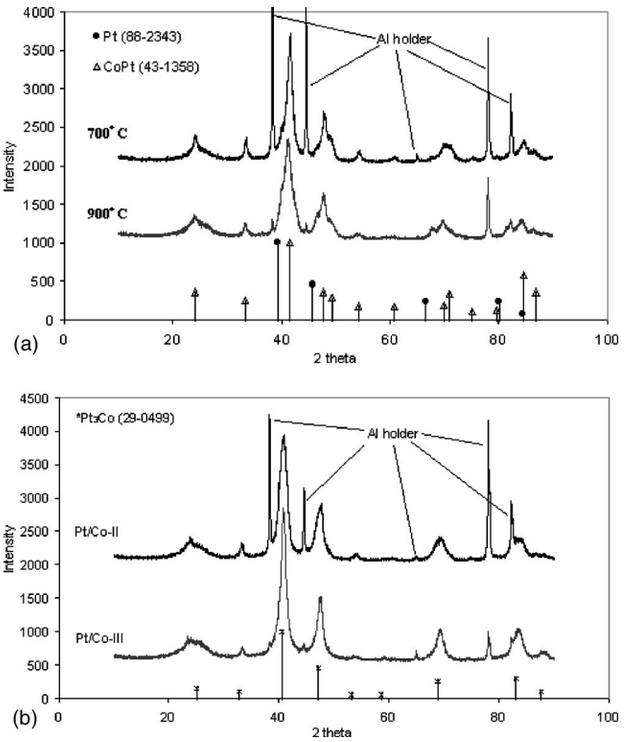

Figure 1. (a) XRD diffraction pattern of Pt/Co-I catalyst material formed by mixing Co oxide sol with Pt/C powder and heat-treating at 700 or 900°C for 2 h. Lines beneath the patterns show reference peaks for (●) pure Pt and (Δ) PtCo alloy.[36] (b) XRD diffraction patterns of Pt/Co-II and Pt/Co-III catalysts formed by mixing [Co,N,C,O] (phen or en) materials with Pt/C powder, followed by heat-treatment for 2 h at 700°C. Lines beneath the pattern show reference peaks for Pt_3Co (*).[37]

Powder X-ray diffraction analysis (XRD).— A Rigaku Multiplex X-ray diffractometer, with an operating voltage of 40 kV and an operating current of 40 mA, was used to collect the spectra. The software for data analysis was Jade 6.5. The powdered samples were placed in shallow Al disk sample holders of 0.5 or 1 mm depth.

Results and Discussion

Characterization of Pt/Co catalyst materials by XRD.— The three Pt/Co catalysts (Table I) were analyzed by XRD to determine their composition. All were found to possess a broad signal centered at a 2θ of 25° due to the presence of carbon powder, while the Pt/C sample also showed the signals for pure Pt, as expected. Also, in many cases, the Al holder contributed to the pattern, as seen by the sharp peaks indicated in Fig. 1.

Starting with Pt/Co-I, formed by mixing the Pt/C powder with the Co oxide sol precursor and heating at either 700 or 900°C, the pattern clearly shows the presence of both pure Pt and a PtCo alloy

(1:1 Pt:Co), as can be seen in Fig. 1a. The particle sizes[d] for both of these phases are small, being ca. 33 and 19 nm for the pure Pt phase for catalysts prepared at 700 and 900°C, respectively, and 12 and 10 nm for the PtCo alloy for these two preparation temperatures. Normally, nanoparticles tend to sinter more at higher temperatures, and as the reverse trend is seen here, this may suggest that somewhat different thermal decomposition processes are occurring at these two temperatures.

Considering the 1:1 ratio of Pt and Co in the original synthesis, the presence of both a PtCo alloy and some pure Pt would lead to the expectation of a signal for metallic Co as well. However, no pure Co metal is detected, suggesting (see below) that Co is present in nanoparticulate form and is therefore not detectable by XRD.

When the Co oxide-en and Co oxide-phen solutions were used as the precursor materials, yielding Pt/Co-II and Pt/Co-III, respectively, the predominant phase present was found to have a different stoichiometry, i.e., Pt_3Co (Fig. 1b). The particle sizes for the Pt/Co-II and Pt/Co-III catalysts were found to be ca. 9 and 10 nm, and 11 and 13 nm, respectively, for the Pt_3Co alloy prepared at 700 and 900°C, respectively. In contrast to Pt/Co-I (above), the expected increase in particle size is seen with increased sintering at higher heat-treatment temperatures. In this case, no obvious lines for pure Pt are seen, and surprisingly, no metallic Co is again detected. In our prior study of the phen- and en-derived precursors alone, in the absence of Pt,[24,26,30] while the samples were seen to be very rich in Co metal by scanning electron microscopy/X-ray photoelectron spectroscopy (SEM/XPS) analysis, no Co metal was detected by XRD. The only possible explanation for this is that the Co particle size in all of these samples is small, i.e., <2 nm, or that an amorphous phase of Co or Co oxide exists[13] such that the Co metal cannot be detected by XRD.

Characterization of Pt/Co ORR catalysts by CV in N_2-purged acid solutions.—Figure 2 shows the CV response of the three main carbon-supported Pt/Co catalysts under study here, Pt/Co-I to -III, as well as of pure Pt/carbon powder and the pure Co oxide sol precursor on carbon (Table I) in a N_2-purged 0.5 M H_2SO_4 solution. These CVs, with the current given per geometric area of the electrode, are for catalysts and precursors heated at 700 and 900°C, respectively, in Fig. 2a and b.

Notably, the CV (Fig. 2a) for the pure Co oxide sol precursor, adsorbed on carbon and then heat-treated at 700°C, demonstrates no particular redox activity and only the relatively featureless response of carbon powder is seen. The CVs for the Pt/carbon powder sample, heated at either 700 or 900°C, exhibit the typical features of Pt, including the hydrogen adsorption/desorption (Hupd) peaks at negative of 0.3 V and the Pt oxide formation/reduction features centered at 0.8 V, all superimposed on the capacitive response of the carbon.

Figure 2a shows that for the three Pt/Co catalysts treated at 700°C, the general characteristics of Pt are still present, although the currents are uniformly lower, regardless of the precursor material employed. Also, the onset of Pt oxide formation is shifted slightly positive vs for Pt/carbon alone. This is similar to what has been reported previously[1] for commercial E-TEK Pt/Co materials. Also, the relative magnitudes and potentials of the Hupd peaks are different for the Pt/Co alloys vs that for Pt. In fact, the potentials of the peaks are generally a little more positive than for pure Pt (the literature reports a mixed trend, depending on which peak is examined[11]). All of these characteristics of the CVs of Pt/Co catalysts vs pure Pt have been reported previously for catalysts obtained commercially (E-TEK)[10] and synthesized metallurgically.[11]

While there is a slightly greater diminishment of the CV currents in the case of the Pt/Co-I catalyst (Pt plus PtCo alloy, Fig. 1) vs at the Pt_3Co materials (as also reported in prior literature[10]), overall,

[d]Crystallite size was determined from the peak width at half height and calculated using the Jade software. Error is estimated at ±1 nm.

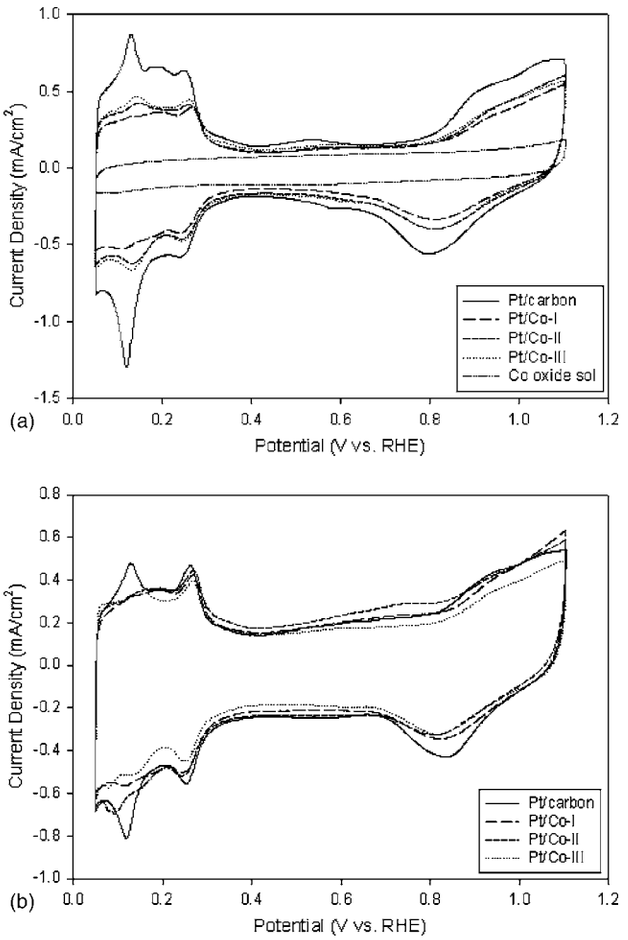

Figure 2. (a) CVs (10 mV/s) collected in room-temperature, N_2-purged 0.5 M H_2SO_4, of the three Pt/Co catalysts, Pt/C alone, and the Co oxide precursor (on carbon powder), all heat-treated for 2 h at 700°C. These materials were coated on a non-rotated GC electrode. (b) CVs (10 mV/s), collected in room-temperature, N_2-purged 0.5 M H_2SO_4, of the three Pt/Co catalysts and Pt/C, heat-treated for 2 h at 900°C. These materials were coated on a non-rotated GC electrode.

these CV responses are similar. While this may not be surprising if the surface of these materials is Pt-rich (considering also the Pt skin model[3,4,11]), these results do rule out any large differences in their real surface area. As well, this shows that the Pt/Co surface sites are not altered, perturbed, or blocked for the ORR as a result of our synthesis.

In the case of the 900°C-heated catalysts, Fig. 2b shows that all of the CVs, including that of Pt/carbon, are almost identical in overall magnitude, indicative of the similar Pt loadings and active surface areas. While it appears from this figure that Pt/Co-III may have a slightly smaller surface area, in most cases, the Hupd peaks have a similar magnitude for both Pt/Co-II and -III. Interestingly, the Hupd peak potentials in Fig. 2b appear to be more different from those at Pt/C alone for the 900°C (vs 700°C) heated materials. There is also clearly less evidence for the presence of sites for weakly adsorbed hydrogen (peak at ca. 0.1 V) at the Co-containing materials vs at pure Pt/C.

All of the Pt/Co catalysts were found to be stable (at least for 30 min of cycling) under acidic conditions, as long as the potential was not extended below 0.0 or above 1.3 V. Therefore, experiments were generally carried out between 0.05 and 1.1 V to prevent any damage or deterioration of these ORR catalysts.

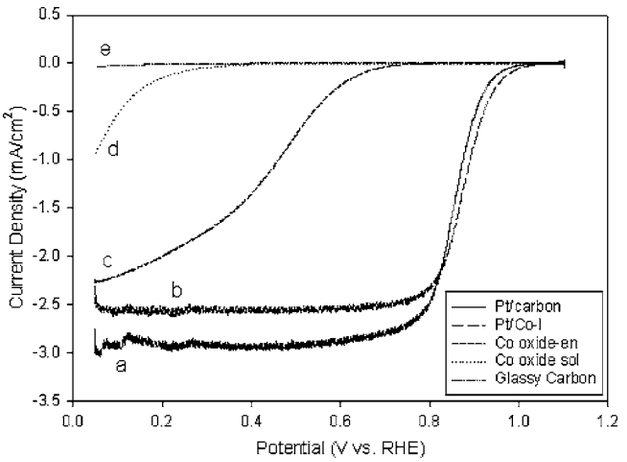

Figure 3. Hydrodynamic voltammetry (10 mV/s, 1000 rpm) of Pt/Co-I catalyst, several precursors, and Pt/C, all heat-treated for 2 h at 900°C (except Co oxide-en, which was heat-treated at 700°C), at GC electrodes in room-temperature, O_2-saturated 0.5 M H_2SO_4: (a) Pt/C, (b) Pt/Co-I, (c) Co oxide-en, (d) Co oxide sol, and (e) GC electrode.

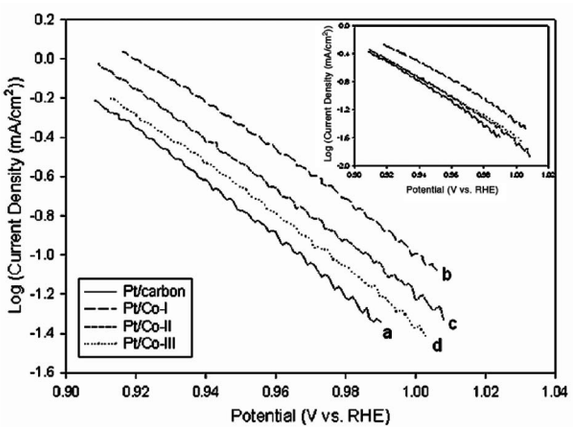

Figure 5. Tafel plots (10 mV/s, 1000 rpm) for the ORR at three Pt/Co catalysts and Pt/C, heat-treated to 900°C, at GC electrodes in room-temperature, O_2-saturated 0.5 M H_2SO_4. The ORR current densities were normalized using the double-layer capacitance measured in N_2-purged solution (see Fig. 3): (a) Pt/C, (b) Pt/Co-I, (c) Pt/Co-II, and (d) Pt/Co-III. Inset: Tafel plots using raw (geometric electrode area) current densities.

O_2 reduction activity of Pt/Co catalysts.— Figure 3 shows the hydrodynamic voltammetric response, corrected for geometric area, for a selection of the carbon-supported Pt/Co catalysts, all in O_2-saturated 0.5 M H_2SO_4 solution. The bare GC electrode (curve e) shows essentially no ORR activity, as expected. In the presence of the Co oxide precursor alone (curve d), only minimal ORR activity is seen, while when the Co oxide-en precursor is examined, the ORR activity is much more substantial.[24,26] The ORR activity shown in curve c is in the range of that observed for thermally decomposed N-containing macrocycles containing Fe or Co.[18,19,24,31]

The key comparison to be made, however, is between the pure Pt/carbon catalysts (curve a) and the sol-derived Pt/Co catalysts (e.g., Pt/Co-I in curve b of Fig. 3). In the activation-controlled region (0.8–1.0 V), these data clearly show that the Pt/Co-I catalyst is notably more active toward the ORR than is pure Pt, when both are supported on carbon. Figure 4 shows a more detailed comparison of the ORR activity of the three Pt/Co catalysts prepared in this work with that of Pt/carbon (all catalysts heat-treated to 900°C). In all cases, the incorporation of Co led to an improvement in the ORR activity above that of Pt/carbon. While our Pt/Co alloys always exhibited higher ORR activities than did pure Pt in the kinetically controlled potential region (0.9–1.0 V), the magnitude of the limiting currents was often somewhat variable. This arises from the fact that after the drying step, our catalyst coatings did not always fully cover the RDE surface, leaving some regions of the GC electrode uncoated. As a result, the projected geometric area of the RDE varied between experiments, thus impacting on the measured current, consistent with the predictions of the Levich equation.[30,32] These nonuniform coatings can also be expected to affect the surface porosity, which is also known to affect limiting current.[30] However, the kinetic region of the I/E response is not affected by any of these coating morphology issues, after correcting for surface area as discussed below. Although not shown in the figures, only trace amounts of hydrogen peroxide were detected by rotating ring disk ellipsometry during oxygen reduction at our Pt/Co catalysts, and *n*, the average number of electrons involved in the ORR, was always greater than 3.9.

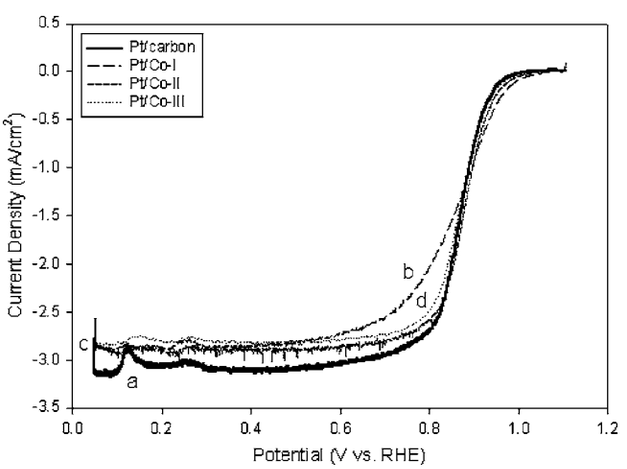

Figure 4. Hydrodynamic voltammetry (10 mV/s, 1000 rpm) of the three Pt/Co catalysts and Pt/C, heat-treated for 2 h at 900°C, at GC electrodes in room-temperature, O_2-saturated 0.5 M H_2SO_4: (a) Pt/C, (b) Pt/Co-I, (c) Pt/Co-II, and (d) Pt/Co-III.

Figure 5 shows the Tafel plots of data obtained in CV experiments, such as shown in Fig. 4, in the potential range between 0.9 and 1.0 V. The raw data, without making any corrections for surface area, are shown in the inset to Fig. 5 for Pt/Co catalysts heat-treated at 900°C. It can be seen that all of the alloy catalysts are more active toward the ORR than pure Pt/C. In this figure (inset, Fig. 5), the best catalyst is the Pt/Co-I catalyst (PtCo alloy) derived from the Co oxide sol precursor.

A visual inspection of the coatings on the GC substrate showed that some catalysts more fully covered the substrate than others. Primarily for this reason, it was considered necessary to examine the trends in activity when the ORR data were normalized for their differences in real surface area. Therefore, both the double-layer capacitance currents in the potential range of 0.35–0.45 V and the Hupd peak charge densities were calculated and assumed to be proportional to the true Pt/Co surface area. The relative ORR current densities for the various catalysts, determined in this way, are shown in Fig. 5. It can be seen that the best ORR catalyst is again the PtCo alloy, arising from the Co oxide sol precursor, while the Pt_3Co alloy, derived from the en and phen precursors (Table I), is less active. This is consistent with the prior literature,[10] which has shown that the 1:1 E-TEK Pt:Co alloy is generally between two and three times more active toward the ORR than the 3:1 alloy material.

Table II provides a summary of the ORR currents at the selected potential of 1.0 V in the activation-controlled region for the various

Table II. Oxygen reduction currents at carbon-supported Pt/Co catalysts and at Pt/carbon, all corrected for real surface area.[a]

Catalyst	Catalyst heat-treatment temperature (°C)	Current density at 1.0 V (mA/cm^2)	Absolute error in current density (mA/cm^2)	Tafel slope (mV/dec) ± 4
Pt/Co-I	700	−0.067	0.01	80
Pt/Co-I	900	−0.094	0.01	84
Pt/Co-II	700	−0.057	-	78
Pt/Co-II	900	−0.068	0.01	81
Pt/Co-III	700	−0.053	0.02	72
Pt/Co-III	900	−0.061	0.02	78
Pt/C	700	−0.033	0.002	67
Pt/C	900	−0.032	0.003	72

[a] Currents converted to current densities using either double-layer capacitance currents or Hupd charge densities (see text for details).

catalysts under study, heat-treated at either 700 or 900°C. The corresponding Tafel slopes are also given for the pure Pt/C and Pt/Co catalysts. It is seen that the same trends in ORR activity hold for both the 700 and 900°C heat-treated catalysts, i.e., Pt/Co-I > Pt/Co-II > Pt/Co-III > Pt/Co. Therefore, PtCo is more active than Pt_3Co, and the Co oxide-en precursor yields a better ORR catalyst than the Co oxide-phen precursor. Also, it can be seen that while the ORR activity appears to be approximately the same for both the 700 and 900°C Pt/C (no Co) catalysts, the Pt/Co catalysts give improved ORR activity at 900 vs 700°C as measured by current density at 1.0 V.

It is also noteworthy that the Pt/Co catalysts proved to be stable in oxygenated 0.5 M H_2SO_4 solution. Over the length of time of electrochemical testing (at least 30 min of continuous cycling), a stable and reproducible ORR response was obtained. As previous work has shown that non-noble metal and alloy catalysts can be unstable under acidic conditions, the stability of our Pt/Co materials, formed via the sol-gel synthesis route, is promising.

Several important questions emerge from this work. A key uncertainty is why the Co oxide precursor results in the formation primarily of the PtCo alloy while the en and phen precursors both produce Pt_3Co. One simple argument could be that the phen and en ligands enhance the binding of Co to the carbon support in the form of C,N-containing surface catalytic sites,[24,26,30] thus leaving less Co available for alloying with Pt. Also, the Co oxide precursor may be more readily thermally decomposed, better allowing the Co to form the PtCo alloy. Another important factor may be the small amount of evaporation of the phen- and en-containing catalysts, which occurs during heat-treatment.[19] During heat-treatment, a precipitate is seen to form on the walls of the quartz tube, most likely due to some Co metal and ligand, thus lowering the Co content and resulting in the formation of the Pt-rich Pt_3Co alloy.

A second question concerns why the 900°C heat-treated Pt/Co catalysts are all more active than those formed at 700°C. For the Pt/Co-I catalyst, this may be related to the unusual diminishment of the alloy particle size (hence increase in area) with temperature, as seen by XRD (Fig. 1).The average particle size for the PtCo phase was 12 and 10 nm for samples prepared at 700 and 900°C, respectively. As argued earlier, the lack of sintering seen here may indicate that the thermal processes occurring during catalyst synthesis are not the same at these two temperatures. For the Pt/Co-II and -III catalysts, the reverse trend is seen. For the Pt/Co-II catalyst, the average particle size was found to be 9 and 10 nm for samples prepared at 700 and 900°C, respectively, while for the Pt/Co-III catalyst, it was 11 and 13 nm at these two heat-treatment temperatures. It has been suggested in the literature that an increase in particle size and subsequent decrease in specific surface area can lead to an increase in activity for Pt catalysts, perhaps due to the increasing exposure of the Pt(100) face.[5] For the Pt/Co-II and -III catalysts this trend is seen, perhaps explaining the catalytic activity of our catalysts. However, for PtCo-I (the Co-oxide derived alloy), the 900°C heat-treated catalyst consists of smaller particles (10 nm PtCo, 19 nm Pt) than the 700°C heat-treated catalyst (12 nm PtCo, 33 nm Pt), and yet it exhibits the higher ORR activity, as shown in Table II.

The improvement in the ORR activity at higher preparation temperatures could also be due to a change in the surface crystallinity, which would affect the ORR activity.[33] Alternatively, it may be due to the reduction of residual PtO_xH_y, which could form spontaneously upon exposure to atmosphere, to Pt metal.[34] This reduction process would occur over the first day or two as a fuel cell is run,[35] and therefore the initial oxidation state of the Pt is generally not of great concern in practice. The absence of any signals for PtO_xH_y in the XRD data may indicate that it is present only as a surface species on the Pt nanoparticles, and thus would not be detectable by XRD.

There is also some evidence that the en-based precursor leads to higher ORR activity vs phen, perhaps due to a stronger binding of Co to phen on the carbon powder surface. This may simply result in less Co free for alloying with Pt in the case of the phen catalyst and thus a lower yield of Pt_3Co. However, more detailed studies of the nature of the surface species present and the identification of the active site are needed to answer this and related questions.

Overall, there are a number of benefits to the Pt/Co alloy synthesis reported in the present work. The sol-gel approach is rapid and facile, with different Pt/Co alloys being formed simply by altering the precursors employed (all at an originally 1:1 ratio of Pt:Co). As well, these catalysts appear to be stable in acidic media, particularly if the upper potential limit is not allowed to exceed 1.3 V. Finally, the activities of the resulting catalysts are all high and exceed the Pt/C standard.

Conclusion

Several Pt/Co-based catalysts for the ORR in PEM fuel cells have been synthesized and characterized in this work. These catalysts were formed by mixing together a Co oxide sol gel or a derivative of this (a Co/N/C material), namely, a sol in which Co is at least partially complexed by ethylenediamine (en) or 1,2-diphenylene (phen), with Pt supported on carbon powder. These catalysts were then heat-treated at either 700 or 900°C prior to electrochemical testing.

The composition of these catalysts has been determined by XRD studies, showing that the Co oxide sol precursor leads to the formation of a PtCo alloy catalyst. When exactly the same procedure was followed using an equivalent molar quantity of a sol-derived Co/N/C catalytic material, Pt_3Co alloy catalysts were formed. XRD data also gave an estimate of the PtCo and Pt_3Co particle sizes, found to be in the range of 9–13 nm.

CV of the resulting alloy catalysts in a N_2-purged 0.5 M H_2SO_4 solution showed strong similarities to the signature of Pt, similar to prior literature reports for these types of Pt/Co alloys. While all of the currents are somewhat lower than at pure Pt on carbon, the magnitude of the CVs are still similar, indicating that the yields and particle sizes are comparable in all cases.

In the presence of oxygen, the PtCo catalysts were found to yield ORR currents approximately 2–3 times vs at pure Pt/C, while the Pt_3Co catalysts yielded enhancements of only factors of ca. 1.5–2. There is also some evidence that the en-based precursor leads to higher ORR activity vs phen, perhaps due to a stronger binding of Co to phen on the carbon powder surface, thus leaving less Co free for alloying with Pt. Notably, the ORR activity of all catalysts under investigation was higher when they were prepared at 900 vs at 700°C. This could be a result of different thermal processes causing a change in the crystal plane or due to differences in the extent of surface oxide, PtO_xH_y, formation.

Overall, the benefits to the Pt/Co alloy synthesis reported in the present work include the fact that the sol-gel approach is rapid and facile, and that different Pt/Co alloys can be formed simply by altering the Co precursors employed (all at an originally 1:1 ratio of

Pt:Co). As well, our catalysts appear to be stable in acidic media, particularly if the upper potential limit is not allowed to exceed 1.3 V.

Acknowledgments

The authors thank the Natural Sciences and Engineering Research Council of Canada for the overall support of this work and also for a post-graduate industrial scholarship to A.H.C.S. and undergraduate scholarship support of J.N.S. We are also grateful to Ballard Power Systems for provision of materials and assistance in the financial support of A.H.C.S. Jingbo (Louise) Lui is gratefully acknowledged for her assistance with the XRD data analysis.

The University of Calgary assisted in meeting the publication costs of this article.

References

1. S. Mukerjee, S. Srinivasn, and M. P. Soriaga, *J. Phys. Chem.*, **99**, 4577 (1995).
2. A. Freund, J. Lang, T. Lehmann, and K. A. Starz, *Catal. Today*, **27**, 279 (1996).
3. T. Toda, H. Igarashi, and M. Watanabe, *J. Electrochem. Soc.*, **145**, 4185 (1998).
4. T. Toda, H. Igarashi, H. Uchida, and M. Watanabe, *J. Electrochem. Soc.*, **146**, 3750 (1999).
5. M. Min, J. Cho, K. Cho, and H. Kim, *Electrochim. Acta*, **45**, 4211 (2000).
6. A. S. Arico, A. K. Shukla, H. Kim, S. Park, M. Min, and V. Antonucci, *Appl. Surf. Sci.*, **172**, 33 (2001).
7. N. M. Markovic, T. J. Schmidt, V. Stamenkovic, and P. N. Ross, *Fuel Cells*, **1**, 105 (2001).
8. M. Neergat, A. K. Shukla, and K. S. Gandhi, *J. Appl. Electrochem.*, **31**, 373 (2001).
9. A. K. Shukla, M. Neergat, P. Bera, V. Jayaram, and M. S. Hegde, *J. Electroanal. Chem.*, **504**, 111 (2001).
10. U. A. Paulus, A. Wokaun, G. G. Scherer, T. J. Schmidt, V. Stamenkovic, V. Radmilovic, N. M. Markovic, and P. N. Ross, *J. Phys. Chem. B*, **106**, 4181 (2002).
11. V. Stamenkovic, T. J. Schmidt, P. N. Ross, and N. M. Markovic, *J. Phys. Chem. B*, **106**, 11970 (2002).
12. M. D. Obradovic, B. N. Grgur, and L. M. Vracar, *J. Electroanal. Chem.*, **548**, 69 (2003).
13. F. H. B. Lima and E. A. Ticianelli, *Electrochim. Acta*, **49**, 4091 (2004).
14. J. Drillet, A. Ea, R. Friedmann, R. Kotz, B. Schnyder, and V. Schmidt, *Electrochim. Acta*, **47**, 1983 (2002).
15. F. J. Luczak and D. A. Landsman, U.S. Pat. 4,677,092 (1985).
16. H. Jahnke, M. Schonborn, and G. Zimmerman, *Top. Curr. Chem.*, **61**, 133 (1976).
17. M. Tsionsky and O. Lev, *J. Electrochem. Soc.*, **142**, 2132 (1995); E. Claude, T. Adduo, J. Latour, and P. Aldebert, *J. Appl. Electrochem.*, **28**, 57 (1997); M. Gokita, M. Yuasa, and I. Sekine, *J. Electrochem. Soc.*, **145**, 815 (1998); C. Contamin, M. Debiemme-Chouvy, M. Savy, and G. Scarbeck, *Electrochim. Acta*, **45**, 721 (1999).
18. G. Lalande, R. Cote, D. Guay, J. Dodelet, L. Weng, and P. Bertrand, *Electrochim. Acta*, **42**, 1379 (1997); M. Lefevre, J. Dodelet, and P. Bertrand, *J. Phys. Chem.*, **104**, 11238 (2000); M. Bron, J. Radnik, M. Fieber-Erdmann, P. Bogdanoff, and S. Fiechter, *J. Electroanal. Chem.*, **535**, 113 (2002); M. Lefevre and J. Dodelet, *Electrochim. Acta*, **48**, 2749 (2003).
19. M. Bron, S. Fiechter, M. Hilgendorff, and P. Bogdanoff, *J. Appl. Electrochem.*, **32**, 211 (2002).
20. W. Seeliger and A. Hamnett, *Electrochim. Acta*, **37**, 763 (1992).
21. G. Lalande, D. Guay, J. Dodelet, S. Majetich, and M. McHenry, *Chem. Mater.*, **9**, 784 (1997).
22. R. Cote, G. Lalande, G. Faubert, D. Guay, J. Dodelet, and G. Denes, *J. New Mater. Electrochem. Syst.*, **1**, 7 (1998).
23. C. Deng and M. Digman, *J. Electrochem. Soc.*, **145**, 3507 (1998);C. Deng and M. Digman, *J. Electrochem. Soc.*, **145**, 3513 (1998).
24. A. Sirk, S. Campbell, and V. Birss, In preparation.
25. A. Sirk, V. Birss, and S. Campbell, in *Proton Conducting Membrane Fuel Cells III*, M. Murthy, T. F. Fuller, J. W. Van Zee, and S. Gottesfeld, Editors, PV2002-31, p. 89, The Electrochemical Society Proceedings Series, Pennington, NJ (2005).
26. A. Sirk, S. Campbell, and V. Birss, *Electrochem. Solid-State Lett.*, **8**, A104 (2005).
27. F. Meaner and N. Lynam, U.S. Pat. 4,959,247 (1990).
28. A. Guerrero-Ruiz, P. Badenes, and I. Rodriguez-Ramos, *Appl. Catal., A*, **173**, 313 (1998); S. Srinivasn, B. Reddy, P. Rao, and A. Rao, in *Recent Developments in Catalysis: Theory and Practice*, B. Viswanathan and C. N. Pillai, Editors, p. 390, Editions Technip, Paris (1992).
29. J. R. C. Salgado, E. Antolini, and E. R. Gonzalez, *J. Electrochem. Soc.*, **151**, A2143 (2004); L. Xiong and A. Manthiram, *Electrochim. Acta*, **50**, 2323 (2005).
30. A. Sirk, Ph.D. Thesis, Department of Chemistry, University of Calgary, Calgary, Alberta, Canada (2004).
31. S. L. Gojkovic, S. Gupta, and R. F. Savinell, *J. Electroanal. Chem.*, **462**, 63 (1999).
32. A. J. Bard and L. R. Faulkner, *Electrochemical Methods: Fundamentals and Applications*, John Wiley & Sons, New York (2001); S. Treimer, A. Tang, and D. C. Johnson, *Electroanalysis*, **14**(3), 165 (2002).
33. J. Bockris and R. Abdu, *J. Electroanal. Chem.*, **448**, 189 (1998).
34. M. Pourbaix, *Atlas of Electrochemical Equilibria in Aqueous Solutions*, National Association of Corrosion Engineers, Houston, TX (1974).
35. R. Viswanathan, G. Hou, R. Liu, S. Bare, F. Modica, G. Mickelson, C. Segre, N. Leyarovska, and E. Smotkin, *J. Phys. Chem.*, **106**, 3458 (2002).
36. Pt: PDF no. 88-2343, CoPt: PDF no. 43-1358 in JCPDS, International Center for Diffraction Files, Swarthmore, PA.
37. Pt_3Co PDF no. 29-0499 in JCPDS, International Center for Diffraction Data Files, Swarthmore, PA.